Analytic description of geometrical spreading in azimuthally anisotropic media

Xiaoxia Xu, Ilya Tsvankin and Andrés Pech
Center for Wave Phenomena, Dept. of Geophysics, Colorado School of Mines, Golden, CO 80401

ABSTRACT
Geometrical spreading is highly sensitive to elastic anisotropy and may strongly influence the amplitude signature of reflected waves recorded over anisotropic formations. For purposes of processing and inversion of reflection data, it is convenient to express geometrical spreading through the reflection traveltime measured at the earth surface. Such expressions are particularly important for azimuthally anisotropic models in which variations of geometrical spreading with both offset and azimuth may significantly distort the results of AVO analysis.
Here, we obtain the inverse geometrical-spreading factor L^{-1} for horizontally layered anisotropic media with a horizontal symmetry plane as a simple function of the spatial derivatives of reflection traveltime. By combining this result with the Tsvankin-Thomsen nonhyperbolic moveout equation, the factor L^{-1} is represented through the moveout coefficients which can be estimated from surface seismic data. This formulation is then applied to P-wave reflections in an othorhombic layer to evaluate the distortions of the geometrical spreading in a typical azimuthally anisotropic model.
The spreading factor L^{-1} in orthorhombic media is controlled by five parameters which are also responsible for time processing of P-wave data: the NMO velocities $V_{\rm nmo}^{(1)}$ and $V_{\rm nmo}^{(2)}$ in the vertical symmetry planes and the anellipticity coefficients $\eta^{(1)}$, $\eta^{(2)}$, and $\eta^{(3)}$. The weak-anisotropy approximation, verified by numerical tests, shows that azimuthal velocity variations make a significant contribution to the geometrical spreading, and the existing VTI equations for the factor L^{-1} cannot be applied even in the vertical symmetry planes. For the $[x_1, x_3]$ symmetry plane, the influence of the azimuthal anisotropy is governed (for weak anisotropy) by the combination $(\eta^{(2)} - \eta^{(1)} + \eta^{(3)})$, and for the $[x_2, x_3]$–plane by $(\eta^{(1)} - \eta^{(2)} + \eta^{(3)})$.
The shape of the azimuthally dependent function L^{-1} is close to an ellipse for offsets smaller than the reflector depth but becomes more complicated for larger offset-to-depth ratios. The overall magnitude of the azimuthal variation of the inverse geometrical spreading for the moderately anisotropic model used in the tests rapidly increases with offset and exceeds 25% for a wide range of offsets. While the formulation developed here is helpful in modeling and analyzing the anisotropic geometrical-spreading factor, its main practical application is in correcting the wide-azimuth AVO signature for the influence of the anisotropic overburden.

Key words: Geometrical spreading, azimuthal anisotropy, wide-azimuth AVO

1 INTRODUCTION

Inversion of prestack amplitude variation with offset and azimuth (AVO analysis) represents one of the most effective tools for characterization of naturally fractured reservoirs. The presence of preferentially oriented fractures and/or horizontal stresses makes the reservoir formation azimuthally anisotropic, and wide-azimuth reflection amplitudes can be used to estimate the fracture orientation and, in some cases, map the lateral variation of the fracture density (Mallick *et al.*, 1998; Lynn *et al.*, 1999; Bakulin *et al.*, 2000; Rüger, 2001). The main advantage of amplitude methods compared to traveltime inversion is their high vertical resolution that makes AVO analysis applicable to relatively thin reservoir layers.

The amplitude signature of reflected waves is controlled by the radiation pattern of the source, geometrical spreading, attenuation, and the reflection/transmission coefficients along the raypath (Martinez, 1993; Maultzsch *et al.*, 2003). Since AVO analysis operates with the reflection coefficient at the target horizon, the critically important element of AVO processing is the removal of the influence of all other factors from the measured amplitude. If the medium does not possess strong attenuation, geometrical spreading makes the most significant contribution to amplitude distortions above the reflector (Martinez, 1993; Ursin & Hokstad, 2002). In particular, if the overburden is anisotropic (as in a sand-shale sequence), it acts like a 3-D focusing lens that changes the amplitude distribution along the wavefront of the reflected wave (Tsvankin, 1995). The results of Tsvankin (1995, 2001) show that for transversely isotropic media the influence of the geometrical spreading on the AVO signature may be comparable to that of the anisotropic term in the reflection coefficient. Therefore, if the overburden contains anisotropic layers, estimation of the reflection coefficient is impossible without an accurate geometrical-spreading correction.

The most straightforward way to compute anisotropic geometrical spreading is by performing dynamic ray tracing (Gajewski & Pšenčík, 1987). For simple homogeneous models it is possible to use analytic approximations of the Green's function, such as that presented by Tsvankin (1995). Using the stationary-phase method and the weak-anisotropy approximation, Tsvankin (1995) obtained explicit expressions for the geometrical spreading and the source directivity factor of P- and SV-waves in a transversely isotropic layer. Modeling methods, however, require accurate information about the anisotropic velocity field for the whole overburden, which is seldom available in practice.

An alternative approach, more suitable for purposes of AVO analysis, is based on relating geometrical spreading to the traveltimes of reflection events recorded at the surface. Ursin & Hokstad (2002) expressed the geometrical spreading in VTI (transversely isotropic media with a vertical symmetry axis) media in terms of the reflection traveltime and the group angle in the subsurface layer. For horizontally layered VTI models, P-wave traveltime can be accurately described by the Tsvankin-Thomsen nonhyperbolic moveout equation (Tsvankin & Thomsen, 1994) parameterized by just two moveout coefficients – the effective NMO velocity $V_{\rm nmo}$ and the effective anellipticity parameter η (Alkhalifah & Tsvankin, 1995). The best-fit parameters $V_{\rm nmo}$ and η can be estimated, for example, by a 2-D semblance scan (Grechka & Tsvankin, 1998), which makes it possible to compute geometrical spreading using solely surface reflection data (Ursin & Hokstad, 2002). This approach can be also used to find analytic expressions for geometrical spreading in terms of the parameters $V_{\rm nmo}$ and η.

The distortions caused by geometrical spreading in reflection amplitudes are even more pronounced for azimuthally anisotropic media (Rüger & Tsvankin, 1997; Maultzsch *et al.*, 2003). Here, we apply ray theory to obtain a general expression for geometrical spreading in terms of reflection traveltime for azimuthally anisotropic models composed of horizontal layers with a horizontal symmetry plane. Substitution of the Tsvankin-Thomsen traveltime equation then yields the geometrical-spreading factor as a function of the azimuthally varying moveout coefficients.

While this result is well-suited for correcting reflection amplitudes for geometrical spreading, the goal of this paper is to evaluate the magnitude of the anisotropic geometrical-spreading factor and its variation with the source-receiver azimuth and the anisotropic parameters. For the model of a single horizontal orthorhombic layer, geometrical spreading is expressed through the medium parameters using the explicit representation of the moveout coefficients given by Al-Dajani *et al.* (1998). Application of the weak-anisotropy approximation helps to explain the dependence of the geometrical-spreading factor on the anisotropic parameters both within and outside the symmetry planes of the model. Numerical tests verify the accuracy of the analytic results and illustrate the character of the amplitude distortions caused by the azimuthally-varying geometrical spreading.

2 GEOMETRICAL SPREADING AS A FUNCTION OF REFLECTION TRAVELTIME

Geometrical spreading is defined as the amplitude decay of an elastic wave caused by the expansion of its wavefront away from the source. The geometrical-spreading factor L can be computed as the ratio of the wavefront curvatures at the source and receiver locations. In the high-frequency limit of the generalized ray approximation, the amplitude along a ray can be written as (Cerveny, 2001; Schleicher *et al.*, 2001):

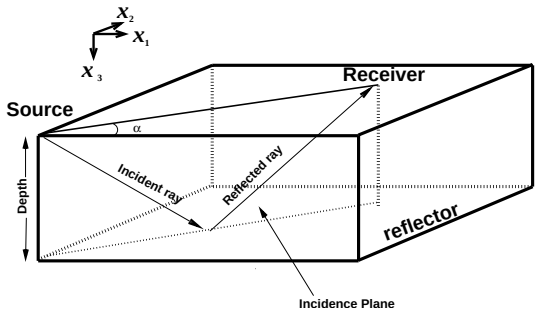

Figure 1. Reflected ray in a horizontal anisotropic layer with a horizontal symmetry plane. The ray lies in the incidence plane, although the corresponding phase-velocity vector may point out of plane.

$$A(x^r,x^s) = \frac{e^{-i\frac{\pi}{2}sgn(w)\kappa(x^r,x^s)}}{4\pi[\rho(x^r)V(x^r)\rho(x^s)V(x^s)]^{1/2}} \times \frac{1}{L(x^r,x^s)}\prod_k R_k \quad , \tag{1}$$

where $L(x^r,x^s)$ is the geometrical spreading between the source location x^s and the receiver location x^r, $\rho(x^s)$ and $V(x^s)$ are the density and group velocity at the source, $\rho(x^r)$ and $V(x^r)$ are the same quantities at the receiver, ω is the circular frequency, $\kappa(x^r,x^s)$ is an index that accounts for possible caustics, and $\prod_k R(k)$ is the product of the plane-wave reflection or transmission coefficients along the raypath. $L(x^r,x^s)$ can be expressed in terms of the second-order traveltime derivatives with respect to the local coordinates associated with the wavefront normal (the normal to the wavefront is parallel to the slowness or phase-velocity vector). Schleicher *et al.* (2001) show that by applying a coordinate rotation, an expression for geometrical spreading can be derived in the so-called "local ray coordinates" associated with the group-velocity vector:

$$L(x^r,x^s) = |\det \boldsymbol{Y}(x^r,x^s)|^{-1/2}\,. \tag{2}$$

The matrix $\boldsymbol{Y}(x^r,x^s)$ is defined as

$$\boldsymbol{Y}(x^r,x^s) = \begin{bmatrix} \frac{\partial^2 T(x^r,x^s)}{\partial g_1^s \partial g_1^r} & \frac{\partial^2 T(x^r,x^s)}{\partial g_1^s \partial g_2^r} \\ \frac{\partial^2 T(x^r,x^s)}{\partial g_2^s \partial g_1^r} & \frac{\partial^2 T(x^r,x^s)}{\partial g_2^s \partial g_2^r} \end{bmatrix}, \tag{3}$$

where T is the traveltime along the ray, g_1^s and g_2^s are the local coordinates in the plane normal to the ray at the source, and g_1^r and g_2^r are the local coordinates defined in the same way at the receiver.

Here, we consider P-wave propagation in a horizontally layered anisotropic medium with a horizontal symmetry plane in each layer (for example, the layers can be orthorhombic). For a single homogeneous layer with a horizontal symmetry plane (Figure 1), the reflected rays are confined to the vertical incidence plane that contains the source and the receiver. Although the rays can deviate from the incidence plane in a multilayered medium, these deviations can usually be ignored for models with moderate azimuthal anisotropy (Al-Dajani and Tsvankin, 1998).

If the incident and reflected rays lie in the incidence plane, it is convenient to rotate the matrix $\boldsymbol{Y}(x^r,x^s)$ from the local ray coordinates into the global Cartesian coordinate system, which results in a matrix denoted by $\boldsymbol{B}$:

$$\boldsymbol{B} = \begin{bmatrix} \frac{\partial^2 T(x^r,x^s)}{\partial x_1^s \partial x_1^r} & \frac{\partial^2 T(x^r,x^s)}{\partial x_1^s \partial x_2^r} \\ \frac{\partial^2 T(x^r,x^s)}{\partial x_2^s \partial x_1^r} & \frac{\partial^2 T(x^r,x^s)}{\partial x_2^s \partial x_2^r} \end{bmatrix} = \boldsymbol{S}\boldsymbol{A}\,\boldsymbol{Y}(x^r,x^r)\,\boldsymbol{R}\,. \tag{4}$$

Here, $\boldsymbol{S}$, $\boldsymbol{A}$, and $\boldsymbol{R}$ are rotation matrices defined as

$$\boldsymbol{S} = \begin{bmatrix} \cos\phi^s & 0 \\ 0 & 1 \end{bmatrix}, \quad \boldsymbol{A} = \begin{bmatrix} \cos\alpha & \sin\alpha \\ -\sin\alpha & \cos\alpha \end{bmatrix}, \quad \text{and} \quad \boldsymbol{R} = \begin{bmatrix} \cos\phi^r & 0 \\ 0 & 1 \end{bmatrix}; \tag{5}$$

ϕ^s and ϕ^r are the angles between the ray and the vertical axis x_3 at the source and receiver locations, respectively, and α is the azimuth of the source-receiver line with respect to the x_1-axis. The matrix $\boldsymbol{A}$ rotates $\boldsymbol{Y}(x^r,x^s)$ around the x_3-axis from the incidence plane to the $[x_1,x_3]$–plane, while $\boldsymbol{S}$ and $\boldsymbol{R}$ rotate $\boldsymbol{Y}(x^r,x^s)$ around the x_2-axis from the local ray coordinates into the Cartesian coordinates x_1 and x_3 at the source and receiver, respectively. From equations (2)–(5) it follows that

$$L(x^r,x^s) = [\cos\phi^s\cos\phi^r]^{1/2}\,|\det\,\boldsymbol{B}|^{-1/2}\,. \tag{6}$$

If the sources and receivers are located on the same horizontal surface, the reflection traveltime depends only on the offset x and the azimuth α of the source-receiver line (Figure 1). Then, as shown in Appendix A, equation (6) becomes the following function of the traveltime T:

$$L(x^r,x^s) = [\cos\phi^s\cos\phi^r]^{1/2} \left[\frac{\partial^2 T}{\partial x^2}\frac{\partial T}{\partial x}\frac{1}{x} + \frac{\partial^2 T}{\partial x^2}\frac{\partial^2 T}{\partial \alpha^2}\frac{1}{x^2} - \left(\frac{\partial T}{\partial \alpha}\right)^2\frac{1}{x^4}\right]^{-1/2} \tag{7}$$

For the special case of a single horizontal layer with a horizontal symmetry plane, the incidence and reflection angles are equal to each other (i.e., $\phi^s = \phi^r = \phi$), and

$$L(x^r,x^s) = \cos\phi \left[\frac{\partial^2 T}{\partial x^2}\frac{\partial T}{\partial x}\frac{1}{x} + \frac{\partial^2 T}{\partial x^2}\frac{\partial^2 T}{\partial \alpha^2}\frac{1}{x^2} - \left(\frac{\partial T}{\partial \alpha}\right)^2\frac{1}{x^4}\right]^{-1/2} \tag{8}$$

Equation (8) not only gives a concise representation of the factor $L(x^r,x^s)$ in terms of the reflection traveltime $T(x,\alpha)$, it also allows us to separate the contributions of azimuthal and polar anisotropy to the geometrical spreading. Indeed, the first term in the brackets coincides with the geometrical spreading factor for VTI media (Ursin & Hostad, 2002), where the traveltime T is independent of the azimuth α. The remaining two terms

in the brackets depend on the azimuthal variation of the traveltime caused by azimuthal velocity anisotropy.

Orthorhombic media with a horizontal symmetry plane have two mutually orthogonal vertical symmetry planes, where the first derivative $\partial T/\partial\alpha$ goes to zero and equation (8) becomes

$$L(x^r, x^s) = \cos\phi \left[\frac{\partial^2 T}{\partial x^2}\frac{\partial T}{\partial x}\frac{1}{x} + \frac{\partial^2 T}{\partial x^2}\frac{\partial^2 T}{\partial \alpha^2}\frac{1}{x^2}\right]^{-1/2}. \quad (9)$$

Equation (9) confirms the conclusion of Tsvankin (1997, 2001) that the kinematic equivalence between the symmetry planes of orthorhombic and VTI media cannot be extended to dynamic properties of the wavefield such as geometrical spreading. The second derivative $\partial^2 T/\partial\alpha^2$, which generally does not vanish even in the symmetry planes, reflects the influence of azimuthal velocity variations on symmetry-plane amplitudes. This 3-D character of geometrical spreading in the symmetry planes is explained by the dependence of the wavefront curvature on both in-plane and out-of-plane (azimuthal) velocity variations. The factor $L(x^r, x^s)$ for source-receiver lines outside the symmetry planes is a function of both the first and second traveltime derivatives with respect to the azimuth α.

3 NONHYPERBOLIC MOVEOUT EQUATION IN ORTHORHOMBIC MEDIA

Reflection moveout, as well as other signatures of reflected waves in orthorhombic media, are convenient to describe using the notation suggested by Tsvankin (1997, 2001). Tsvankin's parameter definitions are based on the analogous form of the Christoffel equation in the symmetry planes of orthorhombic (Figure 2) and VTI media. The anisotropic parameters $\epsilon^{(1)}$, $\delta^{(1)}$, and $\gamma^{(1)}$ play the roles of Thomsen's (1986) VTI coefficients ϵ, δ, and γ in the vertical symmetry plane $[x_2, x_3]$ (the superscript denotes the orthogonal axis x_1). The similar set of the anisotropic coefficients in the $[x_1, x_3]$–plane includes $\epsilon^{(2)}$, $\delta^{(2)}$, and $\gamma^{(2)}$, and one more anisotropic coefficient, $\delta^{(3)}$, is defined in the horizontal plane $[x_1, x_2]$. The parameter V_{P0} denotes the vertical P-wave velocity, and V_{S0} is the velocity of the vertically propagating S-wave polarized in the x_1-direction.

Although orthorhombic symmetry is described by a total of nine independent parameters (for a fixed orientation of the symmetry planes), time-domain signatures of P-waves depend only on five combinations of these parameters. As shown by Grechka and Tsvankin (1999), P-wave reflection traveltimes and the operators for dip-moveout (DMO) correction and time migration in homogeneous orthorhombic media are controlled by the NAM velocities of horizontal events in the vertical

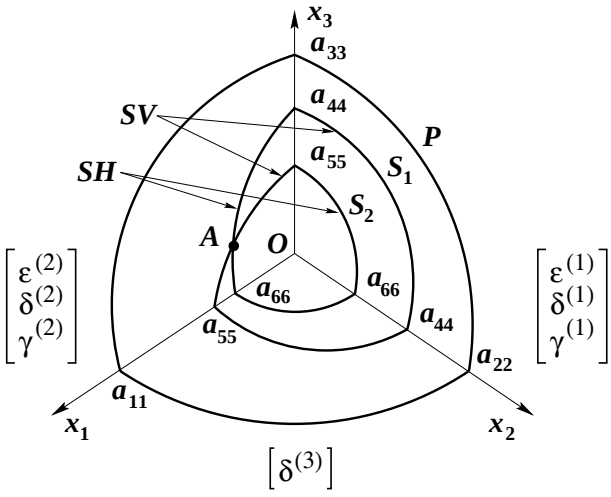

Figure 2. Sketch of body-wave phase-velocity surfaces in orthorhombic media (after Grechka et al., 1999). Tsvankin's (1997) parameters are defined in the mutually orthogonal symmetry planes of the model. *A* marks a point (conical) singularity where the phase velocities of the two S-waves coincide with each other.

symmetry planes, $V_{\rm nmo}^{(1)}$ and $V_{\rm nmo}^{(2)}$, and three anellipticity coefficients defined as follows:

$$\eta^{(1)} \equiv \frac{\epsilon^{(1)} - \delta^{(1)}}{1 + 2\,\delta^{(1)}} \approx \epsilon^{(1)} - \delta^{(1)}\,, \quad (10)$$

$$\eta^{(2)} \equiv \frac{\epsilon^{(2)} - \delta^{(2)}}{1 + 2\,\delta^{(2)}} \approx \epsilon^{(2)} - \delta^{(2)}\,, \quad (11)$$

$$\eta^{(3)} \equiv \frac{\epsilon^{(1)} - \epsilon^{(2)} - \delta^{(3)}\,(1 + 2\epsilon^{(2)})}{(1 + 2\epsilon^{(2)})\,(1 + 2\delta^{(3)})} \approx \epsilon^{(1)} - \epsilon^{(2)} - \delta^{(3)}. \quad (12)$$

To express reflection traveltime and then geometrical spreading through the five time-processing parameters of orthorhombic media, we use the general nonhyperbolic moveout equation suggested by Tsvankin and Thomsen (1994):

$$T^2(x,\alpha) = A_0 + A_2(\alpha)\,x^2 + \frac{A_4(\alpha)\,x^4}{1 + A(\alpha)\,x^2}\,, \quad (13)$$

where

$$A_0 = T_0^2\,, \quad A_2 = \left.\frac{d(T^2)}{d(x^2)}\right|_{x=0}\,,$$

$$\text{and} \quad A_4 = \frac{1}{2}\,\frac{d}{d(x^2)}\left[\frac{d(T^2)}{d(x^2)}\right]\Bigg|_{x=0}\,; \quad (14)$$

T_0 is the zero-offset traveltime, A_2 is related to the normal-moveout (NMO) velocity $V_{\rm nmo}$ as $A_2 = V_{\rm nmo}^{-2}$, and A_4 is the quartic coefficient responsible for nonhyperbolic moveout. The parameter A in the denominator depends on the horizontal group velocity $V_{\rm hor}$ and is designed to make $T(x)$ convergent at large offsets $x \to \infty$ (Tsvankin and Thomsen, 1994):

$$A = \frac{A_4}{V_{\rm hor}^{-2} - V_{\rm nmo}^{-2}}\,. \quad (15)$$

The general form of equation (13) makes it sufficiently accurate for P-wave moveout in models with substantial azimuthal anisotropy, provided the azimuthal variation of A_2, A_4, and A is taken into account (Al-Dajani & Tsvankin, 1998; Al-Dajani *et al.*, 1998).

For P-waves in VTI media, the parameters A_2, A_4, and A can be expressed through the NMO velocity of horizontal events,

$$V_{\rm nmo} = V_{P0}\sqrt{1+2\delta}\,, \tag{16}$$

and the anellipticity parameter η,

$$\eta \equiv \frac{\epsilon-\delta}{1+2\delta}\,. \tag{17}$$

Equation (13) then reduces to the form given by Alkhalifah and Tsvankin (1995):

$$T^2(x) = T_0^2 + \frac{x^2}{V_{\rm nmo}^2} - \frac{2\eta\,x^4}{V_{\rm nmo}^2\,[T_0^2\,V_{\rm nmo}^2 + (1+2\eta)\,x^2]}\,. \tag{18}$$

As shown below, equation (18) can be extended in a straightforward way to a weakly anisotropic orthorhombic layer.

For orthorhombic media, the hyperbolic coefficient A_2 was obtained by Grechka and Tsvankin (1998a), who proved that the azimuthal variation of NMO velocity has a simple elliptical form even in arbitrarily anisotropic, heterogeneous media. Since an orthorhombic layer has two orthogonal vertical symmetry planes, the axes of the NMO ellipse should be aligned with the symmetry-plane directions, which yields (for P-waves):

$$A_2(\alpha) = A_2^{(1)}\sin^2\alpha + A_2^{(2)}\cos^2\alpha\,, \tag{19}$$

$$A_2^{(1)} = \frac{1}{[V_{\rm nmo}^{(1)}]^2} = \frac{1}{V_{P0}^2\,(1+2\delta^{(1)})}\,, \tag{20}$$

$$A_2^{(2)} = \frac{1}{[V_{\rm nmo}^{(2)}]^2} = \frac{1}{V_{P0}^2\,(1+2\delta^{(2)})}\,; \tag{21}$$

α is the azimuth with respect to the x_1-axis.

The azimuthally dependent P-wave quartic moveout coefficient A_4 was derived by Al-Dajani et al. (1998) as

$$A_4(\alpha) = A_4^{(1)}\sin^4\alpha + A_4^{(2)}\cos^4\alpha + A_4^{(x)}\sin^2\alpha\,\cos^2\alpha\,, \tag{22}$$

$$A_4^{(1)} = \frac{-2\eta^{(1)}}{T_0^2\,[V_{\rm nmo}^{(1)}]^4}\,, \tag{23}$$

$$A_4^{(2)} = \frac{-2\eta^{(2)}}{T_0^2\,[V_{\rm nmo}^{(2)}]^4}\,, \tag{24}$$

$$A_4^{(x)} = \frac{2}{T_0^2\,[V_{\rm nmo}^{(1)}]^2\,[V_{\rm nmo}^{(2)}]^2} \left[1-\sqrt{\frac{(1+2\eta^{(1)})\,(1+2\eta^{(2)})}{1+2\eta^{(3)}}}\right]\,, \tag{25}$$

where $A_4^{(1)}$ and $A_4^{(2)}$ are the symmetry-plane coefficients and $A_4^{(x)}$ is a cross-term that contributes to nonhyperbolic moveout in off-symmetry directions.

While equation (13) with the moveout coefficients listed above provides an accurate description of long-spread moveout, it is too complicated to elucidate the dependence of geometrical spreading on the anisotropic parameters. A simplified form of equation (13) can be obtained by assuming that the magnitude of velocity anisotropy is weak and employing the approximate kinematic equivalence between vertical planes in orthorhombic and VTI media. As discussed by Tsvankin (2001, p. 164), in the limit of weak anisotropy all out-of-plane phenomena in a horizontal orthorhombic layer can be ignored. Also, the P-wave phase velocity in any vertical plane of orthorhombic media can be described by Thomsen's (1986) VTI equation with azimuthally-dependent coefficients ϵ and δ. Therefore, P-wave reflection moveout in a horizontal orthorhombic layer can be approximated by the VTI equation (18) with the appropriate parameters $V_{\rm nmo}$ and η for each azimuth:

$$T^2(x,\alpha) = T_0^2 + \frac{x^2}{V_{\rm nmo}^2(\alpha)} - \frac{2\eta(\alpha)\,x^4}{V_{\rm nmo}^2(\alpha)\,[T_0^2\,V_{\rm nmo}^2(\alpha) + (1+2\eta(\alpha))\,x^2]}\,. \tag{26}$$

In equation (26), $V_{\rm nmo}(\alpha)$ is determined from equations (19)–(21),

$$V_{\rm nmo}^2(\alpha) = \frac{[V_{\rm nmo}^{(1)}]^2\,[V_{\rm nmo}^{(2)}]^2}{[V_{\rm nmo}^{(1)}]^2\cos^2\alpha + [V_{\rm nmo}^{(2)}]^2\sin^2\alpha}\,, \tag{27}$$

and the azimuthally dependent η is given by (Pech and Tsvankin, 2003)

$$\eta(\alpha) = \eta^{(1)}\sin^2\alpha - \eta^{(3)}\sin^2\alpha\,\cos^2\alpha + \eta^{(2)}\cos^2\alpha\,. \tag{28}$$

Although the linearization in the anisotropic parameters implied by the weak-anisotropy approximation requires dropping the coefficient $\eta(\alpha)$ from the denominator of equation (26), the complete denominator of the original VTI equation (18) can be retained to increase the accuracy at large source-receiver offsets.

4 GEOMETRICAL-SPREADING FACTOR IN AN ORTHORHOMBIC LAYER

The derivatives of the traveltime with respect to offset and azimuth needed to obtain the geometrical spreading $L(x^r, x^s)$ from equation (8) can be found using the nonhyperbolic moveout equation (13). Explicit expressions for the traveltime derivatives in terms of the azimuthally dependent moveout coefficients A_2, A_4, and A are given in Appendix B. Substitution of equations (19), (22), and (15) for $A_2(\alpha)$, $A_4(\alpha)$, and $A(\alpha)$ yields the geometrical spreading factor as a function of the parameters of orthorhombic media. Equation (8) also contains the term $\cos\phi$ (ϕ is the group angle) that can be written as $(T_0\,V_{P0})/\sqrt{x^2 + T_0^2\,V_{P0}^2}$. The final equation for the geometrical-spreading factor, which is too lengthy

to be included in the paper, is used in the numerical tests below.

While the derived expression is well-suited for numerical modeling of the factor $L(x^r, x^s)$, it does not provide insight into the dependence of the geometrical spreading on the anisotropic parameters. Therefore, next we apply the weak-anisotropy approximation based on equation (26) to obtain the inverse geometrical-spreading factor $L^{-1}(x^r, x^s)$:

$$L^{-1}(x^r, x^s) = \cos^{-1}\phi \left[\frac{\partial^2 T}{\partial x^2}\frac{\partial T}{\partial x}\frac{1}{x} + \frac{\partial^2 T}{\partial x^2}\frac{\partial^2 T}{\partial \alpha^2}\frac{1}{x^2} - \left(\frac{\partial T}{\partial \alpha}\right)^2 \frac{1}{x^4}\right]^{1/2} \quad (29)$$

The traveltime derivatives in equation (29) are found from equation (26) and then linearized in the anellipticity parameters $\eta^{(1,2,3)}$. Further linearization of equation (29) gives the weak-anisotropy approximation for $L^{-1}(x^r, x^s)$ analyzed below.

5 ANALYSIS OF THE WEAK-ANISOTROPY APPROXIMATION

5.1 Geometrical spreading in the symmetry planes

While the full linearized expression for geometrical spreading is still rather long, it takes a much more concise form in the vertical symmetry planes. For the symmetry plane $[x_1, x_3]$, we find

$$L^{-1} = \cos^{-1}\phi \, \frac{A + Bx^2 + Cx^4}{V^{(1)}_{\rm nmo} V^{(2)}_{\rm nmo} (T_0^2 [V^{(2)}_{\rm nmo}]^2 + x^2)^3}, \quad (30)$$

where

$$\cos\phi = \frac{T_0 V_{P0}}{\sqrt{x^2 + T_0^2 V_{P0}^2}}, \quad (31)$$

$$A = T_0^5 \left[V^{(2)}_{\rm nmo}\right]^6, \quad (32)$$

$$B = T_0^3 \left[V^{(2)}_{\rm nmo}\right]^2 \left\{2\left[1 - 4\eta^{(2)}\right]\left[V^{(2)}_{\rm nmo}\right]^2 + \left[\eta^{(2)} + \eta^{(3)} - \eta^{(1)}\right]\left[V^{(1)}_{\rm nmo}\right]^2\right\} \quad (33)$$

$$C = T_0 \left\{\left[1 + \eta^{(2)}\right]\left[V^{(2)}_{\rm nmo}\right]^2 + \left[\eta^{(2)} + \eta^{(3)} - \eta^{(1)}\right]\left[V^{(1)}_{\rm nmo}\right]^2\right\}. \quad (34)$$

.

For the single-layer model, the term $\cos^{-1}\phi$ in equation (30) is purely isotropic and, for fixed values of the zero-offset time T_0 and offset x, depends just on the vertical velocity V_{P0}.

At zero offset, the factor L^{-1} becomes $1/(T_0 V^{(1)}_{\rm nmo} V^{(2)}_{\rm nmo})$, which is an exact expression that can be obtained directly from the wavefront curvatures for any strength of the anisotropy. From equations (20) and (21) for the NMO velocities it is clear that the geometrical spreading at vertical incidence is governed by two anisotropic coefficients, $\delta^{(1)}$ and $\delta^{(2)}$, which also determine the NMO ellipse. For VTI media, $V^{(1)}_{\rm nmo} = V^{(2)}_{\rm nmo}$, and L^{-1} at zero offset reduces to $1/(T_0 V^2_{\rm nmo})$; this result was previously obtained by Tsvankin (1995) and Ursin & Hostad (2002). If the medium is isotropic, L^{-1} further simplifies to the well-known expression $1/(T_0 V_{P0}^2)$.

The factors B and C in equation (30) can be called the "near-offset" and "far-offset" spreading coefficients, respectively. It should be emphasized that B and C include terms dependent on both in-plane and out-of-plane traveltime (and, therefore, velocity) variations. P-wave reflection traveltime in the incidence plane is controlled just by the NMO velocity $V^{(2)}_{\rm nmo}$ and the anisotropic parameter $\eta^{(2)}$ (Grechka and Tsvankin, 1999, Tsvankin, 2001). Hence, the term $(1-4\eta^{(2)})\,[V^{(2)}_{\rm nmo}]^2$ in the coefficient B represents the in-plane contribution that coincides with the corresponding (near-offset) spreading factor for VTI media. The other term in the expression for B, $(eta^{(2)} - \eta^{(1)} + \eta^{(3)})\,[V^{(1)}_{\rm nmo}]^2$, is entirely due to azimuthal anisotropy and a nonzero value of the second traveltime derivative with respect to α. Similarly, the far-offset coefficient C contains the in-plane term $(1+\eta^{(2)})\,[V^{(2)}_{\rm nmo}]^2$ and exactly the same out-of-plane term as the one in the expression for B.

The inverse spreading factor L^{-1} in the symmetry plane $[x_2, x_3]$ can be obtained from equation (30) by simply switching the superscripts (1) and (2) in the NMO velocities and the coefficients η. A more detailed comparison of the geometrical spreading in the symmetry planes of orthorhombic media with that in VTI media is given in the numerical examples below.

5.2 Azimuthal variation of geometrical spreading

Since azimuthal AVO analysis often operates with prestack amplitudes measured at a fixed offset, it is of interest to analyze the azimuthally-varying spreading factor $L^{-1}(\alpha)$ for x = const. To facilitate the analysis of the function $L^{-1}(\alpha)$, it is convenient to replace the NMO velocities in the hyperbolic moveout term of equation (26) with their expressions in terms of the coefficients $\delta^{(1)}$ and $\delta^{(2)}$. Linearizing both the x^2- and x^4-terms in equation (26) in the anisotropic parameters yields

$$T^2(\alpha, x) = T_0^2 + x^2 \frac{1 - \delta^{(1)} - \delta^{(2)} + (\delta^{(2)} - \delta^{(1)})\cos 2\alpha}{V_{P0}^2} - 2x^4 \frac{\eta^{(2)}\cos^2\alpha + \eta^{(1)}\sin^2\alpha - \eta^{(3)}\cos^2\alpha\,\sin^2\alpha}{T_0^2 V_{P0}^4 (1 + \frac{x^2}{T_0^2 V_{P0}^2})}. \quad (35)$$

Substituting the moveout equation (35) into equation (29) and carrying out further linearization in the anisotropic parameters, we obtain the inverse geometrical spreading as

$$L^{-1}(x,\phi) = D(x) \quad + \quad E(\alpha)\left[\frac{x}{T_0\,V_{P0}}\right]^2 + \quad F(\alpha)\left[\frac{x}{T_0\,V_{P0}}\right]^4 + \ldots \qquad (36)$$

Here, $D(x)$ is an azimuthally-independent term that would coincide with L^{-1} in VTI media if the anisotropic coefficients in the vertical symmetry planes were identical, and $\eta^{(3)} = 0$. The azimuthally-varying terms were expanded in x^2, and powers of x higher than four were neglected. The coefficients E and F are given by

$$E(\alpha) = T_0^2\,V_{P0} \left\{3\left[\eta^{(1)} - \eta^{(2)}\right] - \left[\delta^{(1)} - \delta^{(2)}\right]\right\}\cos 2\alpha; \qquad (37)$$

$$F(\alpha) = T_0^2\,V_{P0}\left\{\left[\frac{3}{2}(\delta^{(1)} - \delta^{(2)}) + 9(\eta^{(1)} - \eta^{(2)})\right] \cos 2\alpha + \frac{9}{8}\eta^{(3)}\cos 4\alpha\right\}. \qquad (38)$$

The coefficient $E(\alpha)$ in equation (37) determines the azimuthal dependence of the geometrical spreading at near offsets. Since $E(\alpha)$ is proportional to $\cos 2\alpha$, for small x the function $L^{-1}(\alpha)$ traces out a curve close to an ellipse. In contrast, the far-offset coefficient F contains both $\cos 2\alpha$ and $\cos 4\alpha$, and the form of $L^{-1}(\alpha)$ may substantially deviate from elliptical; this is illustrated by numerical examples in the next section. The magnitude of the azimuthal variation of geometrical spreading is controlled by the differences $(\delta^{(1)} - \delta^{(2)})$, $(\eta^{(1)} - \eta^{(2)})$ and, at far offsets, by the coefficient $\eta^{(3)}$. If $\delta^{(1)} = \delta^{(2)}$, $\eta^{(1)} = \eta^{(2)}$, and $\eta^{(3)} = 0$, P-wave velocity becomes azimuthally independent, and for purposes of computing P-wave geometrical spreading the orthorhombic medium becomes equivalent to VTI.

6 NUMERICAL EXAMPLES

The numerical tests presented here are designed to illustrate the following properties of the inverse geometrical-spreading factor L^{-1} in an orthorhombic layer:

- The influence of azimuthal anisotropy on L^{-1} in the vertical symmetry planes.
- The azimuthal variation of L^{-1} at a fixed source-receiver offset.
- The spatial variation of L^{-1} plotted as a function of offset and azimuth.
- The accuracy of the weak-anisotropy approximation for L^{-1}.

In the examples below we use an orthorhombic model formed by parallel vertical penny-shaped cracks embedded in a VTI background. The stiffness coefficients for this model are given in Schoenberg and Helbig (1997), and the corresponding anisotropic parameters, listed in the caption of Figure 3, are taken from Tsvankin (1997). Although this model has substantial azimuthal velocity variations, it is dominated by the VTI component, with both ϵ coefficients close to 30%.

As before, we assume that the coordinate planes coincide with the symmetry planes of the orthorhombic layer. The inverse geometrical spreading factor L^{-1} is computed using both the "exact" formalism and the weak-anisotropy approximation. The "exact" approach is based on combining equation (29) for L^{-1} with the Tsvankin-Thomsen moveout equation [using equations (19), (22), and (15) for the moveout coefficients] without making any approximations in computing the traveltime derivatives and the spreading factor itself. The word "exact" is put in quotes because the Tsvankin-Thomsen equation, despite its high accuracy for P-waves, is not an exact representation of the reflection traveltime. The weak-anisotropy approximation, as described in the previous section, is obtained by linearizing all equations in the anisotropic coefficients.

The inverse geometrical-spreading factor L^{-1} in the vertical symmetry planes of the model is displayed in Figure 3. In addition to the "exact" (solid line) and weak-anisotropy (dashed line) solutions, we plot the "exact" values of L^{-1} for the reference VTI models (dotted line) in each symmetry plane. The reference VTI model has the same vertical velocity V_{P0} as the actual orthorhombic medium and the anisotropic parameters ϵ and δ equal to the corresponding parameters in a given symmetry plane. For example, the reference VTI parameters for the $[x_1, x_3]$ symmetry plane are $\epsilon = \epsilon^{(2)}$ and $\delta = \delta^{(2)}$.

All three curves are normalized by the factor L^{-1} in the corresponding isotropic model with the velocity V_{P0}. Clearly, the influence of anisotropy leads to significant distortions of geometrical spreading in a wide range of offsets for both symmetry planes. As shown by Tsvankin (1995, 2001) for VTI media, the influence of anisotropy causes the amplitude (e.g., the inverse geometrical-spreading factor) to decrease away from the vertical if the difference $\epsilon - \delta$ is positive (i.e., $\eta > 0$). Figure 3 confirms that this conclusion remains valid for the symmetry planes of orthorhombic media with moderate azimuthal anisotropy. Indeed, the η coefficients in both vertical symmetry planes ($\eta^{(1)}$ and $\eta^{(2)}$) are positive, and the normalized factor L^{-1} rapidly decreases with offset at near-vertical incidence.

Comparison with the geometrical spreading in the reference VTI medium helps to quantify the influence of azimuthal anisotropy in both symmetry planes. It is interesting that azimuthal anisotropy changes the geometrical-spreading factor even at vertical incidence, where for orthorhombic media $L^{-1} = 1/(T_0\,V_{\rm nmo}^{(1)}\,V_{\rm nmo}^{(2)})$, while for VTI media $L^{-1} = 1/(T_0\,V_{\rm nmo}^2)$. If we substi-

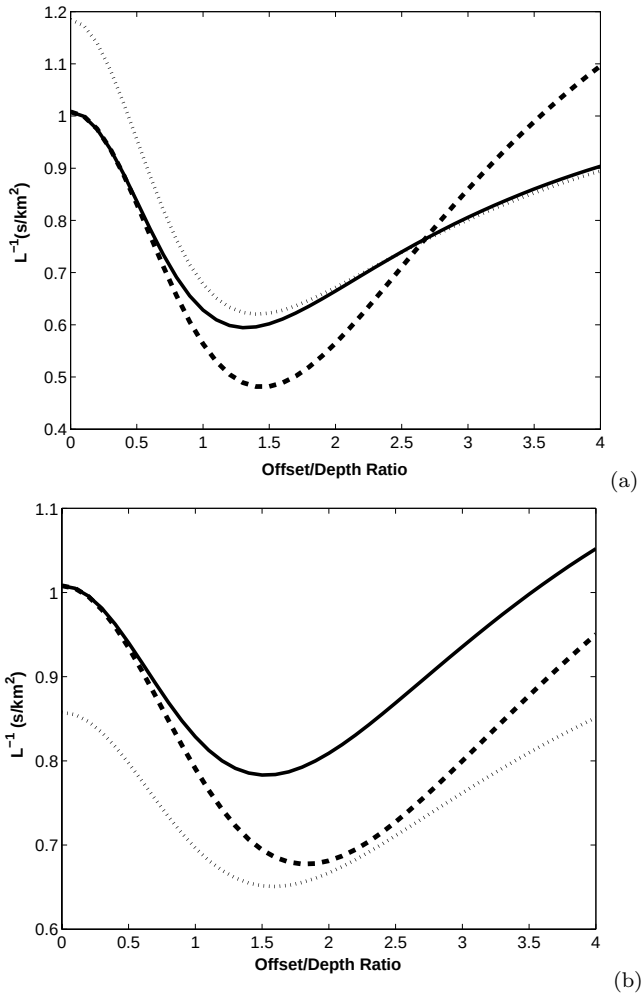

Figure 3. Inverse geometrical spreading L^{-1} as a function of the offset-to-depth ratio in the symmetry planes $[x_1, x_3]$ (a) and $[x_2, x_3]$ (b) of a horizontal orthorhombic layer. The solid line is the "exact" result, the dashed line is the weak-anisotropy approximation, and the dotted line is L^{-1} in the reference VTI model (see the main text for explanation). The model parameters are $V_{P0} = 2.437$ km/s, $\epsilon^{(1)} = 0.329$, $\epsilon^{(2)} = 0.258$, $\delta^{(1)} = 0.083$, $\delta^{(2)} = -0.078$, and $\delta^{(3)} = -0.106$. The corresponding P-wave time-processing parameters are $V_{\rm nmo}^{(1)} = 2.632$ km/s, $V_{\rm nmo}^{(2)} = 2.239$ km/s, $\eta^{(1)} = 0.211$, $\eta^{(2)} = 0.398$, and $\eta^{(3)} = 0.193$. The factor L^{-1} is normalized by its value in the corresponding isotropic layer with the velocity $V_{P0} = 2.437$ km/s.

tute the NMO velocity in the $[x_1, x_3]$ symmetry plane into the VTI expression, we get a value that is 18% larger than the actual L^{-1} (Figure 3a), while for the $[x_2, x_3]$ symmetry plane the VTI result is 15% smaller (Figure 3b).

As follows from the weak-anisotropy approximation discussed in the previous section, the influence of azimuthal velocity variations on the offset-dependent part of the factor L^{-1} in the $[x_1, x_3]$ symmetry plane is controlled by the combination $(\eta^{(2)} - \eta^{(1)} + \eta^{(3)})$ of the anellipticity coefficients. Since for our model this combination is positive and relatively large (0.38), L^{-1} in the $[x_1, x_3]$ plane initially decreases with offset slower than in the corresponding VTI media (Figure 3a). For offset-to-depth ratios exceeding two, however, the factor L^{-1} almost coincides with the VTI value, which contradicts the weak-anisotropy result.

Similarly, the factor L^{-1} in the $[x_2, x_3]$ symmetry plane contains the "out-of-plane" term proportional to $(\eta^{(1)} - \eta^{(2)} + \eta^{(3)})$. For the model at hand, however, this term is close to zero (0.006), and the offset dependence of the geometrical spreading in the $[x_2, x_3]$–plane is close to that in the reference VTI medium (Figure 3b).

Figure 3 also helps to evaluate the accuracy of the weak-anisotropy approximation for a model that can be characterized as moderately-to-strongly anisotropic in terms of the magnitude of P-wave velocity variations. While the weak-anisotropy solution is exact at zero offset (because we did not linearize the NMO velocities in the denominator of the hyperbolic term of L^{-1}), it rapidly deviates from the exact factor L^{-1} with increasing offset. Still, the weak-anisotropy approximation correctly predicts the general character of the function $L^{-1}(x)$ and remains accurate for offset-to-depth ratios of up to about one.

The azimuthal variation of the normalized factor L^{-1} at two different offsets is plotted in Figure 4. Since the geometrical spreading in an orthorhombic layer is symmetric with respect to both vertical coordinate planes, the signature of L^{-1} is repeated in each quadrant. For the offset equal to the reflector depth, the azimuthal variation of L^{-1} is close to elliptical, as predicted by the weak-anisotropy approximation (Figure 4a). The fractional difference of L^{-1} between the symmetry planes, which determines the overall magnitude of the azimuthal variation of the inverse geometrical spreading, is about 30%. Hence, for this model the eccentricity of the "geometrical-spreading ellipse" exceeds that of the NMO ellipse (18%). For larger offset-to-depth ratios, the shape of the curve $L^{-1}(\alpha)$ becomes more complicated and, in agreement with the weak-anisotropy approximation (38) for the x^4–term, deviates from an ellipse (Figure 4b). The magnitude of the azimuthal variation of $L^{-1}(\alpha)$ does not noticeably increase with offset for offset-to-depth ratios between one and two.

A complete picture of the spatial variations of the geometrical spreading in our model is given in Figure 5a, where the factor L^{-1} is computed as a function of both offset and azimuth. The combined influence of polar and azimuthal anisotropy creates a rather complicated pattern of the normalized factor L^{-1}, with substantial azimuthal variations and pronounced deviations from the corresponding isotropic values. The largest anisotropy-induced distortions of the geometrical spreading reach-

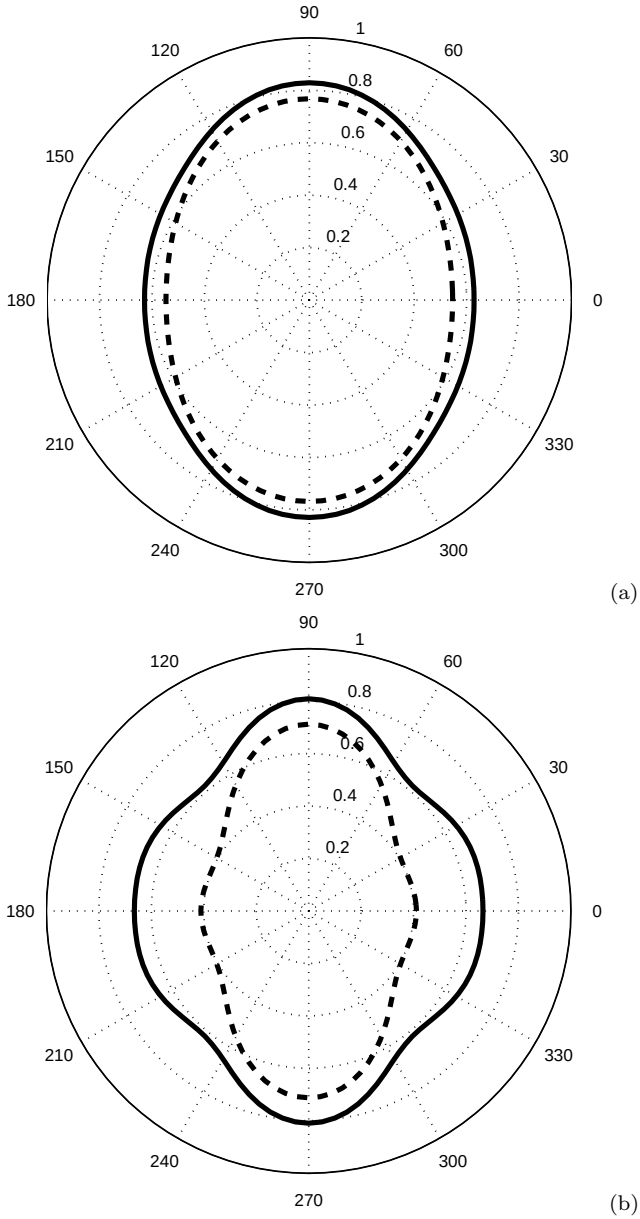

Figure 4. Azimuthal variation of the normalized factor L^{-1} for offset-to-depth ratios of one (a) and two (b). The azimuth α (numbers on the perimeter) is measured with respect to the x_1-axis. The solid line is the "exact" solution, the dashed line is the weak-anisotropy approximation.

ing 40% are observed near the $[x_1, x_3]$–plane for offset-to-depth ratios of about 1.5.

The significant azimuthal variation of L^{-1} at near offsets is partly caused by the opposite signs of the δ coefficients in the vertical symmetry planes. In Figure 5b we changed the sign of $\delta^{(2)}$ (the other model parameters remained the same), which reduced the differences between the symmetry-plane NMO velocities $[V^{(1)}_{\rm nmo}$ and $V^{(2)}_{\rm nmo}]$ and between the corresponding η coefficients $[\eta^{(1)}$ and $\eta^{(2)}]$. Although the symmetry-plane factors L^{-1} did become close at near offsets, the azimuthal variation of L^{-1} at far offsets is not much smaller than it was for the original model in Figure 5a.

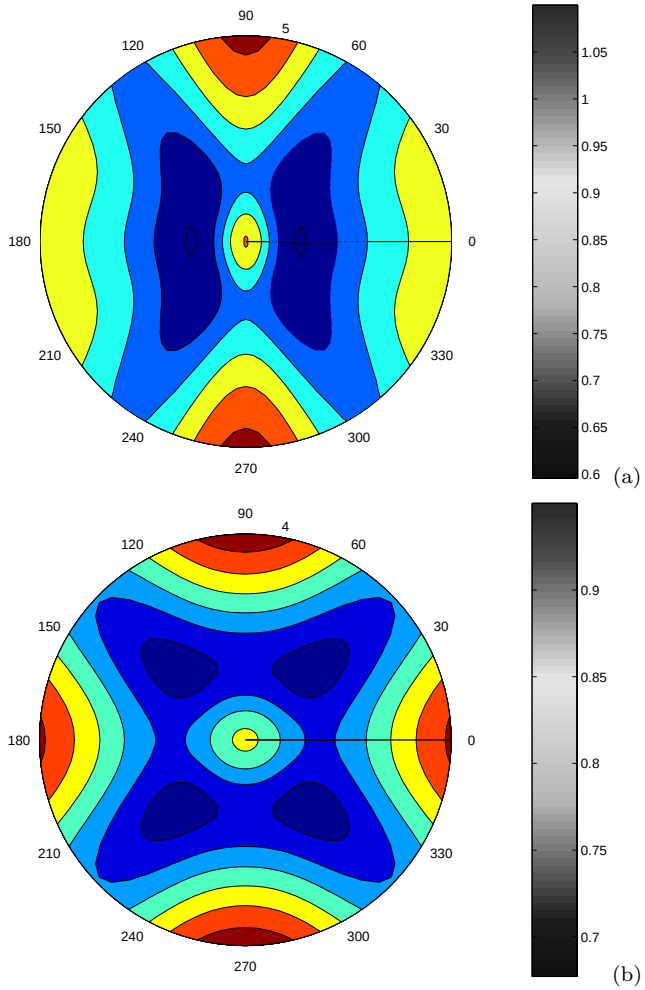

Figure 5. Map of the normalized factor L^{-1} as a function of offset and azimuth. The offset-to-depth ratio varies from zero to four. The model in plot (a) is the same as that in Figures 3 and 4; in plot (b), the sign of the parameter $\delta^{(2)}$ was changed from negative to positive (i.e., $\delta^{(2)} = 0.078$).

7 DISCUSSION AND CONCLUSIONS

Although geometrical spreading of reflected waves is determined by the medium properties along the whole raypath, it can be obtained from the reflection traveltime and the group angles at the surface. We showed that for a stack of horizontal azimuthally anisotropic layers with a horizontal symmetry plane, the inverse geometrical-spreading factor L^{-1} can be expressed as a simple function of the traveltime derivatives with

respect to offset and azimuth. Describing the traveltime by the Tsvankin-Thomsen nonhyperbolic moveout equation (Tsvankin and Thomsen, 1994) helps to represent the factor L^{-1} through the azimuthally varying moveout coefficients.

For a horizontal orthorhombic layer, the factor L^{-1} was related to the medium parameters by using the explicit expressions for the moveout coefficients given by Al-Dajani et al. (1998). P-wave traveltime and, therefore, the geometrical spreading for this model is governed by the NMO velocities $V_{\rm nmo}^{(1)}$ and $V_{\rm nmo}^{(2)}$ in the vertical symmetry planes and the anellipticity coefficients $\eta^{(1)}$, $\eta^{(2)}$, and $\eta^{(3)}$. To explain the dependence of the factor L^{-1} on these parameters, we employed the weak-anisotropy approximation based on linearization in the anisotropic coefficients. The analytic results were verified by numerical tests for an orthorhombic model formed by vertical penny-shaped cracks embedded in a VTI matrix.

Although the geometrical-spreading signature in a single orthorhombic layer is repeated in each quadrant, the variation of the factor L^{-1} with offset and azimuth has a rather complicated character. For the model used here, the error of the isotropic equation for the geometrical spreading reaches a maximum of 40% in the intermediate offset range (i.e., for the offset-to-depth ratio between one and two). The azimuthal variation $L^{-1}(\alpha)$ for a fixed offset is close to elliptical at relatively small offsets-to-depth ratios close to one. For larger offsets, $L^{-1}(\alpha)$ deviates from an ellipse and may have intermediate minima or maxima between the symmetry planes.

Both analytic and numerical results show that the spreading factor L^{-1} is substantially influenced by azimuthal velocity variations even in the vertical symmetry planes. At zero offset (vertical incidence), the exact inverse geometrical spreading is given by a simple equation that involves only the NMO velocities in both symmetry planes: $L^{-1} = 1/(T_0\, V_{\rm nmo}^{(1)}\, V_{\rm nmo}^{(2)})$. The offset-dependent part of L^{-1} in the symmetry planes can be separated (in the weak-anisotropy approximation) into the in-plane term, identical to the factor L^{-1} in the corresponding VTI medium, and the out-of-plane term associated with azimuthal anisotropy. In the $[x_1, x_3]$–plane, the contribution of azimuthal velocity variation is proportional to the combination $(\eta^{(2)} - \eta^{(1)} + \eta^{(3)})$, and in the $[x_2, x_3]$–plane to $(\eta^{(1)} - \eta^{(2)} + \eta^{(3)})$.

The large magnitude of the anisotropy-induced distortions of the factor L^{-1} means that reliable interpretation of the AVO response for media with azimuthally anisotropic overburden is impossible without properly correcting for the geometrical spreading. The estimation and removal of geometrical spreading can be accomplished by applying the Tsvankin-Thomsen moveout equation with fitted (i.e., estimated from the data) coefficients. The methodology of the geometrical-spreading correction for azimuthally anisotropic media will be discussed in a sequel paper.

ACKNOWLEDGMENTS

We are grateful to Matt Haney for his careful review of the manuscript and to Debashish Sarkar for his help in using LaTeXand xfig. Partial support for this work was provided by the Chemical Sciences, Geosciences and Biosciences Division, Office of Basic Energy Sciences, U.S. Department of Energy.

REFERENCES

Al-Dajani, A., & Tsvankin, I. 1998. Nonhyperbolic reflection moveout for horizontal transverse isotropy. *Geophysics*, **63**, 1738–1753.

Al-Dajani, A., Tsvankin, I., & Toksoz, N. 1998. Nonhyperbolic reflection moveout for azimuthally anisotropic media. *68th Ann. Internat. Mtg., Soc. Expl. Geophys., Expanded Abstracts*, 1479–1482.

Alkhalifah, T., & Tsvankin, I. 1995. Velocity analysis for transversely isotropic media. *Geophysics*, **60**, 1550–1566.

Bakulin, A., Grechka, V., & Tsvankin, I. 2000. Estimation of fracture parameters from reflection seismic data–Part I: HTI model due to a single fracture set. *Geophysics*, **65**, 1788–1802.

Cerveny, V. 2001. *Seismic ray theory*. Cambridge University Press.

Gajewski, D., & Pšenčík, I. 1987. Computation of high frequency seismic wavefields in 3-D laterally inhomogeneous anisotropic media. *Geophys. J. R. Astr. Soc.*, **91**, 383–412.

Grechka, V., & Tsvankin, I. 1998. Feasibility of nonhyperbolic moveout inversion in transversely isotropic media. *Geophysics*, **63**, 957–969.

Grechka, V., & Tsvankin, I. 1999. 3-D moveout velocity analysis and parameter estimation for orthorhombic media. *Geophysics*, **64**, 820–837.

Lynn, H.B., Campagna, D., Simon, K.M., & Beckham, W.E. 1999. Relationship pf P-wave seismic attributes, azimuthal anisotropy, and commercial gas pay in 3-D P-wave multiazimuth data, Rulison Field, Piceance Basin, Colorado. *Geophysics*, **64**, 1312–1328.

Mallick, S., Craft, K., & Meister, L. 1998. Determination of the principal directions of azimuthal anisotropy from P-wave seismic data. *Geophysics*, **63**, 692–706.

Martinez, R.D. 1993. Wave propagation effects on amplitude variation with offset measurements: A modeling study. *Geophysics*, **58**, 534–543.

Maultzsch, S., Horne, S., Archer, S., & Burkhardt, H. 2003. Effects of an anisotropic overburden on azimuthal amplitude analysis in horizontal transverse isotropic media. *Geophysics Prospecting*, **51**, 61–74.

Rüger, A. 2001. *Reflection coefficients and azimuthal AVO analysis in anisotropic media*. Society of Exploration Geophysics.

Rüger, A., & Tsvankin, I. 1997. Using AVO for fracture detection: Analytic basis and practical solutions. *The Leading Edge*, **16**, 1429–1434.

Schleicher, J., Tygel, M., Ursin, B., & Bleistein, N. 2001. The Kirchhoff-Helmholtz integral for anisotropic elastic media. *Wave Motion*, **34**, 353–364.

Thomsen, L. 1986. Weak elastic anisotropy. *Geophysics*, **51**, 1954–1966.

Tsvankin, I. 1995. Body-wave radiation patterns and AVO in transversly isotropic media. *Geophysics*, **60**, 1409–1425.

Tsvankin, I. 1997. Anisotropic parameters and P-wave velocity for orthorhombic media. *Geophysics*, **62**, 1292–1309.

Tsvankin, I., & Thomsen, L. 1994. Nonhyperbolic reflection moveout in anisotropic media. *Geophysics*, **59**, 1290–1304.

Ursin, B., & Hokstad, K. 2002. Geometrical spreading in a layered transversely isotropic medium with vertical symmetry axis. *CWP annual report*, 97–107.

APPENDIX A: GEOMETRICAL SPREADING OVER AN AZIMUTHALLY ANISOTROPIC MEDIUM WITH A HORIZONTAL SYMMETRY PLANE

As shown in the main text [equation (6)], the geometrical-spreading factor for a stack of horizontal anisotropic layers with a horizontal symmetry plane can be written in the following form:

$$L(x^r, x^s) = [\cos\phi^s \cos\phi^r]^{1/2} \, |\det \boldsymbol{B}|^{-1/2} \,, \tag{A1}$$

where

$$\boldsymbol{B} = \begin{bmatrix} \frac{\partial^2 T(x^r,x^s)}{\partial x_1^s \partial x_1^r} & \frac{\partial^2 T(x^r,x^s)}{\partial x_1^s \partial x_2^r} \\ \frac{\partial^2 T(x^r,x^s)}{\partial x_2^s \partial x_1^r} & \frac{\partial^2 T(x^r,x^s)}{\partial x_2^s \partial x_2^r} \end{bmatrix} . \tag{A2}$$

When the source and receiver lie on the same horizontal surface, the traveltime T depends only on the distance x between the source and the receiver and the azimuth α of the source-receiver line with respect to the x_1-axis:

$$x = \sqrt{(x_1^r - x_1^s)^2 + (x_2^r - x_2^s)^2} \,, \tag{A3}$$

$$\alpha = \tan^{-1}\left[\frac{x_2^r - x_2^s}{x_1^r - x_1^s}\right] . \tag{A4}$$

If the traveltime T is expressed as a function of x and α, the elements of the matrix $\boldsymbol{B}$ become

$$\frac{\partial^2 T}{\partial x_1^s \partial x_1^r} = \frac{\partial^2 T}{\partial x^2}\frac{\partial x}{\partial x_1^s}\frac{\partial x}{\partial x_1^r} + \frac{\partial T}{\partial x}\frac{\partial^2 x}{\partial x_1^s \partial x_1^r} + \frac{\partial^2 T}{\partial \alpha^2}\frac{\partial \alpha}{\partial x_1^s}\frac{\partial \alpha}{\partial x_1^r} + \frac{\partial T}{\partial \alpha}\frac{\partial^2 \alpha}{\partial x_1^s \partial x_1^r} \,, \tag{A5}$$

$$\frac{\partial^2 T}{\partial x_1^s \partial x_2^r} = \frac{\partial^2 T}{\partial x^2}\frac{\partial x}{\partial x_1^s}\frac{\partial x}{\partial x_2^r} + \frac{\partial T}{\partial x}\frac{\partial^2 x}{\partial x_1^s \partial x_2^r} + \frac{\partial^2 T}{\partial \alpha^2}\frac{\partial \alpha}{\partial x_1^s}\frac{\partial \alpha}{\partial x_2^r} + \frac{\partial T}{\partial \alpha}\frac{\partial^2 \alpha}{\partial x_1^s \partial x_2^r} \,, \tag{A6}$$

$$\frac{\partial^2 T}{\partial x_2^s \partial x_1^r} = \frac{\partial^2 T}{\partial x_1^s \partial x_2^r} \,, \tag{A7}$$

$$\frac{\partial^2 T}{\partial x_2^s \partial x_2^r} = \frac{\partial^2 T}{\partial x^2}\frac{\partial x}{\partial x_2^s}\frac{\partial x}{\partial x_2^r} + \frac{\partial T}{\partial x}\frac{\partial^2 x}{\partial x_2^s \partial x_2^r} + \frac{\partial^2 T}{\partial \alpha^2}\frac{\partial \alpha}{\partial x_2^s}\frac{\partial \alpha}{\partial x_2^r} + \frac{\partial T}{\partial \alpha}\frac{\partial^2 \alpha}{\partial x_2^s \partial x_2^r} \,. \tag{A8}$$

The derivatives of x and α with respect to the source and receiver coordinates can be obtained from equations (A3) and (A4):

$$\frac{\partial x}{\partial x_i^s} = \frac{x_i^s - x_i^r}{x} \,, \frac{\partial x}{\partial x_i^r} = \frac{x_i^r - x_i^s}{x} \,, \quad (i = 1, 2) \tag{A9}$$

$$\frac{\partial \alpha}{\partial x_1^s} = \frac{x_2^r - x_2^s}{x^2} \,, \quad \frac{\partial \alpha}{\partial x_2^s} = \frac{x_1^s - x_1^r}{x^2} \,, \tag{A10}$$

$$\frac{\partial \alpha}{\partial x_1^r} = \frac{x_2^s - x_2^r}{x^2} \,, \quad \frac{\partial \alpha}{\partial x_2^r} = \frac{x_1^r - x_1^s}{x^2} \,, \tag{A11}$$

$$\frac{\partial^2 x}{\partial x_1^s \partial x_1^r} = \frac{-(x_2^r - x_2^s)^2}{x^3} \,, \tag{A12}$$

$$\frac{\partial^2 x}{\partial x_1^s \partial x_2^r} = \frac{(x_1^r - x_1^s)(x_2^r - x_2^s)}{x^3} \,, \tag{A13}$$

$$\frac{\partial^2 x}{\partial x_2^s \partial x_2^r} = \frac{-(x_1^r - x_1^s)^2}{x^3} \,, \tag{A14}$$

$$\frac{\partial^2 \alpha}{\partial x_1^s \partial x_1^r} = \frac{-2(x_1^r - x_1^s)(x_2^r - x_2^s)}{x^4} \,, \tag{A15}$$

$$\frac{\partial^2 \alpha}{\partial x_1^s \partial x_2^r} = \frac{(x_1^r - x_1^s)^2 - (x_2^r - x_2^s)^2}{x^4} \,, \tag{A16}$$

$$\frac{\partial^2 \alpha}{\partial x_2^s \partial x_2^r} = \frac{2(x_1^r - x_1^s)(x_2^r - x_2^s)}{x^4} \,. \tag{A17}$$

Substituting equations (A9)–(A17) into equations (A5)–(A8) yields

$$\frac{\partial^2 T}{\partial x_1^s \partial x_1^r} = -\frac{\partial^2 T}{\partial x^2}\frac{(x_1^r - x_1^s)^2}{x^2} - \frac{\partial T}{\partial x}\frac{(x_2^r - x_2^s)^2}{x^3} - \frac{\partial^2 T}{\partial \alpha^2}\frac{(x_2^r - x_2^s)^2}{x^4} - \frac{\partial T}{\partial \alpha}\frac{2(x_1^r - x_1^s)(x_2^r - x_2^s)}{x^4} \,, \tag{A18}$$

$$\frac{\partial^2 T}{\partial x_1^s \partial x_2^r} = \frac{\partial^2 T}{\partial x^2}\frac{-(x_1^r - x_1^s)(x_2^r - x_2^s)}{x^2} + \frac{\partial T}{\partial x}\frac{(x_1^r - x_1^s)(x_2^r - x_2^s)}{x^3} \tag{A19}$$

$$+ \frac{\partial^2 T}{\partial \alpha^2}\frac{(x_1^r - x_1^s)(x_2^r - x_2^s)^2}{x^4} + \frac{\partial T}{\partial \alpha}\frac{(x_1^r - x_1^s)^2 - (x_2^r - x_2^s)^2}{x^4}\,, \tag{A20}$$

$$\frac{\partial^2 T}{\partial x_2^s \partial x_2^r} = -\frac{\partial^2 T}{\partial x^2}\frac{(x_2^r - x_2^s)^2}{x^2} - \frac{\partial T}{\partial x}\frac{(x_1^r - x_1^s)^2}{x^3} - \frac{\partial^2 T}{\partial \alpha^2}\frac{(x_1^r - x_1^s)^2}{x^4} + \frac{\partial T}{\partial \alpha}\frac{2(x_1^r - x_1^s)(x_2^r - x_2^s)}{x^4}\,. \tag{A21}$$

The determinant of the matrix $\boldsymbol{B}$ is then found as

$$\det|\boldsymbol{B}| = \frac{\partial^2 T}{\partial x^2}\frac{\partial T}{\partial x}\frac{1}{x} + \frac{\partial^2 T}{\partial x^2}\frac{\partial^2 T}{\partial \alpha^2}\frac{1}{x^2} - \left(\frac{\partial T}{\partial \alpha}\right)^2\frac{1}{x^4}\,. \tag{A22}$$

Finally, using equation (A22), the geometrical-spreading factor (A1) can be expressed through the traveltime derivatives with respect to the offset x and azimuth α:

$$L(x^r, x^s) = (\cos\phi^s \cos\phi^r)^{1/2}\left[\frac{\partial^2 T}{\partial x^2}\frac{\partial T}{\partial x}\frac{1}{x} + \frac{\partial^2 T}{\partial x^2}\frac{\partial^2 T}{\partial \alpha^2}\frac{1}{x^2} - \left(\frac{\partial T}{\partial \alpha}\right)^2\frac{1}{x^4}\right]^{-1/2}. \tag{A23}$$

APPENDIX B: TRAVELTIME DERIVATIVES FROM THE NONHYPERBOLIC MOVEOUT EQUATION

P-wave nonhyperbolic (long-spread) reflection traveltime can be accurately described by the Tsvankin-Thomsen (1994) moveout equation:

$$T^2(x,\alpha) = T_0^2 + A_2(\alpha)\,x^2 + \frac{A_4(\alpha)\,x^4}{1 + A(\alpha)\,x^2}\,, \tag{B1}$$

where the moveout coefficients A_2, A_4, and A generally vary with the azimuth α.

The derivatives of the traveltime with respect to the offset x are given by

$$\frac{\partial T}{\partial x} = \frac{1}{T}\left[A_2 x + \frac{2A_4 x^3}{1 + Ax^2} - \frac{AA_4 x^5}{(1 + Ax^2)^2}\right] \tag{B2}$$

and

$$\frac{\partial^2 T}{\partial x^2} = \frac{1}{T}\left[f(x) - \left(\frac{\partial T}{\partial x}\right)^2\right]; \tag{B3}$$

$$f(x) \equiv A_2 + \frac{6A_4 x^2}{1 + Ax^2} - \frac{9AA_4 x^4}{(1 + Ax^2)^2} + \frac{4A_4 A^2 x^6}{(1 + Ax^2)^3}\,. \tag{B4}$$

Differentiating equation (B1) with respect to azimuth yields

$$\frac{\partial T}{\partial \alpha} = \frac{1}{2T}\left[A_2' x^2 + \frac{A_4' x^4}{1 + Ax^2} - \frac{A_4 A' x^6}{(1 + Ax^2)^2}\right] \tag{B5}$$

and

$$\frac{\partial^2 T}{\partial \alpha^2} = \frac{\partial T}{\partial \alpha}\frac{1}{2T^2}\left[A_2' x^2 + \frac{A_4' x^4}{1 + Ax^2} - \frac{A_4 A' x^6}{(1 + Ax^2)^2}\right] + \frac{1}{2T}\left[A_2'' x^2 + \frac{A_4'' x^4}{1 + Ax^2} - \frac{A_4 A'' x^6}{(1 + Ax^2)^2} - \frac{2A' A_4' x^6}{(1 + Ax^2)^2} + \frac{2A_4 A'^2 x^8}{(1 + Ax^2)^3}\right]. \tag{B6}$$

Here, A_2', A_4', A', A_2'', A_4'' and A'' are the first and second derivatives of the moveout coefficients with respect to α. For the model of a single orthorhombic layer, these derivatives can be found from the explicit expressions for A_2, A_4, and A given in the main text.